Zero Field Splitting Parameters of Fe^{3+} doped $Cs_2NaAl_3F_{12}$ Single Crystal

Ram Kripal

EPR Laboratory, Department of Physics, University of Allahabad, Allahabad-211002, India

Abstract

Zero field splitting parameters (ZFSPs) D and E of Fe^{3+} doped $Cs_2NaAl_3F_{12}$ (CSA) single crystals are evaluated theoretically at room temperature (RT) employing crystal field parameters (CFPs) from superposition model. The D and E thus determined show reasonable agreement with the experimental values. The experimental inference that Fe^{3+} substitutes for Al^{3+} in CSA is well supported by this study. The zero field splitting parameters D and E are calculated without and with local distortion. These D and E show reasonable agreement with the experimental ones when the local distortion is taken into account.

Keywords: A. Inorganic compounds; A. Single crystal; D. Crystal fields; D. Optical properties; D. Electron paramagnetic resonance.

I. Introduction

Electron paramagnetic resonance (EPR) is used to find local site symmetry and zero field splitting parameters (ZFSPs) of transition ions doped in crystals [1, 2]. Fe^{3+} ion in the iron group with spin S = 5/2 has the ground state ^6S. The electron spins affected by the crystal field through high order interaction freely orient in the external magnetic field.

The superposition model (SPM) gives physical and geometrical information included in crystal field parameters and assumes that the spin Hamiltonian parameters result from contribution of each nearest neighbor of the paramagnetic ion [3, 4]. The positions of various ligands in the crystal should be known to apply this model. Hence, the theories of local distortion in crystals are very important.

Theoretical studies of spin Hamiltonian parameters of d^5 ions have been carried out by many workers [5-7]. Various mechanisms have been suggested to contribute to the ground state splitting of the paramagnetic ions in crystals [8]. The effect of spin Hamiltonian is, in general, studied by perturbation methods. In most of the systems, cubic field and the diagonal part of free-ion Hamiltonian are taken as unperturbed terms while the spin-orbit coupling, the low-symmetry field, and the off-diagonal part of free-ion Hamiltonian are assumed as the perturbation terms [9].

EPR absorption of Fe^{3+} doped $Cs_2NaAl_3F_{12}$ (CSA) single crystals has been done earlier [10]. Two possibilities exist for Fe^{3+} site in the CSA crystal, substitutional and interstitial. It is interesting to find the site of the impurity in CSA crystal. It was suggested [10] that Fe^{3+} ion substitutes at Al^{3+} site in CSA lattice. In this study, the zero-field splitting parameters (ZFSPs) D and E are determined for the Fe^{3+} ion at substitutional Al^{3+} site in CSA; employing crystal field parameters (CFPs) obtained from superposition model and perturbation theory [11]. The objective of study is to find whether Fe^{3+} ion enters the crystal lattice substitutionally or interstitially and also about the distortion in the lattice. The results obtained from this model yield reasonable agreement with the experimental ones when the local distortion for the Fe^{3+} ion at substitutional Al^{3+} site in CSA crystal is taken into account.

II. Crystal Structure

The crystal structure of $Cs_2NaAl_3F_{12}$ (CSA) crystal is trigonal (rhombohedral) having unit cell parameters a = 0.7310 nm, α = 57.450, space group $R\bar{3}m$ and Z = 1 [12]. The structure is built with $(AlF_4^-)_n$ layers perpendicular to the trigonal axis. The orientations of the *(x, y, z)* axes (SAAS-symmetry adopted axis system) relative to the *(a, b, c)* crystallographic axes are *(x → a, y → b, z → c)* as shown in Fig. 1.

III.   Theoretical Investigation

The experimental resonance magnetic fields are analyzed with the help of the spin Hamiltonian [13, 14] for orthorhombic symmetry,

$$\mathcal{H} = \mu_B B.g.S + D\left\{S_Z^2 - \frac{1}{3}S(S+1)\right\} + E(S_x^2 - S_y^2) + \frac{a}{6}[S_x^4 + S_y^4 + S_Z^4 - \frac{1}{5}S(S+1)(3S^2 + 3S + 1)] \tag{1}$$

where g is the spectroscopic splitting factor, μ_B is the Bohr magneton and B is the external magnetic field. D and E are the second rank axial and rhombic ZFSPs, whereas *a* is the fourth rank cubic ZFSP [15, 16]. The maximum overall splitting of the EPR spectrum is taken along the z axis and the minimum along the x axis [17]. The laboratory axes (x, y, z) are parallel to the crystallographic axes. The local site symmetry axes, i. e. the symmetry adopted axes (SAA) are the nearly orthogonal directions of metal-ligand bonds. The Z-axis of SAAS is coincident with the crystal **c**-axis and the other two axes (X, Y) lie in the ab plane (Fig. 1). This indicates that Fe^{3+} substitutes Al^{3+} in the crystal lattice. The ionic radius of Fe^{3+} ion 0.064 nm [18] is slightly larger as compared to the ionic radius of Al^{3+} (0.054 nm), thus Fe^{3+} ion can substitute at the site of Al^{3+} with some distortion.

The ZFSPs of Fe^{3+} ions are determined using the perturbation theory [19, 20]. These values are then compared with the experimental ones.

The spin Hamiltonian of a d^5 (^{6}S state) ion may be written as sum of free ion ($\mathcal{H}_o$), spin-orbit coupling ($\mathcal{H}_{so}$), spin-spin coupling ($\mathcal{H}_{ss}$) and crystal field ($\mathcal{H}_c$) Hamiltonians,

$$\mathcal{H} = \mathcal{H}_o + \mathcal{H}_{so} + \mathcal{H}_{ss} + \mathcal{H}_c \tag{2}$$

$$\text{where} \quad \mathcal{H}_c = \sum B_{kq} C_q^{(k)} \tag{3}$$

The B_{kq} are the crystal-field parameters and $C_q^{(k)}$ are the Wybourne spherical tensor operators. For the orthorhombic symmetry crystal field, $B_{kq} \neq 0$ only with k = 2, 4, q = 0, 2, 4. The crystal-field theory has been largely used for the study of spin Hamiltonian parameters of transition ions doped in various crystals [11, 21-23]. In our study, we have calculated the CFPs, B_{kq} using SPM [19].

In CSA crystal the local symmetry around Fe^{3+} ions is considered to be orthorhombic of type I (OR-I) [10, 18]. In OR-I symmetry, the ZFSPs D and E are given by [11]

$$D^{(4)}(SO) = \left(\frac{3\xi^2}{70P^2D}\right)[-B_{20}^2 - 21\xi B_{20} + 2B_{22}^2] + \left(\frac{\xi^2}{63P^2G}\right)[-5B_{40}^2 - 4B_{42}^2 + 14B_{44}^2] \tag{4}$$

$$E^{(4)}(SO) = \left(\frac{\sqrt{6}\xi^2}{70P^2D}\right)[2B_{20} - 21\xi]B_{22} + \left(\frac{\xi^2}{63P^2G}\right)[3\sqrt{10}B_{40} + 2\sqrt{7}B_{44}]B_{42} \tag{5}$$

where P = 7B+7C, G = 10B+5C, D = 17B+5C. B and C are Racah parameters, giving electron-electron repulsion and ξ is the spin-orbit coupling parameter. It is found that the values of B and C for transition metal ion in a crystal are less than those of the free ion. By considering the average covalency parameter N, we can write the Racah parameters [19, 24] and spin-orbit coupling parameter as B = N^{4}B$_0$, C = N^4 C$_0$, ξ = N$^2\xi_0$, where B$_0$ and C$_0$ are Racah parameters for free ion and ξ_0 is free ion spin-orbit coupling parameter. For free Fe^{3+}ion, B$_0$ = 1130 cm^{-1}, C$_0$ = 4111 cm^{-1} and ξ_0 = 589 cm^{-1} are used [19].
Taking the values of Racah parameters (B = 899 cm^{-1}, C = 3198 cm^{-1}) obtained from optical study of the Fe^{3+} ion with F ligand [25], the average parameter N is obtained from N = ($\sqrt{B/B_0} + \sqrt{C/C_0}$)/2.

The CFPs from SPM are written [11, 26] as

$$B_{kq} = \sum_j \overline{A_k}(R_j) K_{kq}(\theta_j, \phi_j) \tag{6}$$

where the co-ordination factor $K_{kq}(\theta_j, \varphi_j)$ is an explicit function of the angular position of the ligand. The intrinsic parameter $\overline{A_k}(R_j)$ is given as

$$\overline{A_k}(R_j) = \overline{A_k}(R_0)\left(\frac{R_0}{R_j}\right)^{t_k}$$

where R_j is the distance between the d^n ion and the ligand, $\overline{A_k}(R_0)$ gives the intrinsic parameter of the reference crystal, t_k is the power law exponent and R_0 is the reference distance between metal and ligand. For Fe^{3+} doped in various crystals having different ligands, $t_2 = 3$ and $t_4 = 5$ [23]. The above values are used here in our calculation. Since the co-ordination around Fe^{3+} ion is octahedral, $\overline{A_4}$ and Dq are related as [27]

$$\overline{A_4}(R_0) = \frac{3}{4}Dq$$

From optical study [25], the value of $Dq = 1390$ cm⁻¹. Hence, the relation gives the value of $\overline{A_4}(R_0) = 1042.5$ cm⁻¹. It is found that for $3d^5$ ions the ratio of $\overline{A_2}(R_0)$ and $\overline{A_4}(R_0)$ lies between 8 to 12 [19, 28, 29]. In the present study, $\dfrac{\overline{A_2}}{\overline{A_4}} = 10$ is taken, which gives $\overline{A_2} = 10425$ cm⁻¹.

IV. Results and Discussion

The CFPs B_{kq} of Fe^{3+} ion in CSA are calculated using SPM with the help of parameters $\overline{A_2}$ and $\overline{A_4}$ and arrangement of ligand ions about Fe^{3+} ion (Fig. 1). Atomic coordinates in CSA crystal and bond length R (without and with distortion) along with angle θ, φ (one site) are shown in Table 1. The calculated CFPs with transformation S5 for standardization [17] and ZFSPs together with reference distance R_0 are given in Table 2. It is seen from Table 2 that the value of $R_0 = 0.108$ nm slightly less than the lowest of four ligand distances from the central metal ion (0.1747 nm) together with local distortion give ZFSPs in reasonable agreement with the experimental values [10]. The ZFSPs calculated using $R_0 = 0.108$ nm and without local distortion are quite larger than the experimental values. For comparison the interstitial sites for Fe^{3+} ions were also calculated. The calculated values of ZFSPs are found to be different from the experimental ones and hence are not provided here.

Employing CFPs and CFA program [30, 31] with OR-I symmetry of the crystal field the optical spectra of Fe^{3+} doped CSA crystals are calculated. The energy levels of the impurity ion are found by diagonalization of the complete Hamiltonian within the $3d^N$ basis of states in the intermediate crystal field coupling scheme. The calculated energy values are shown in Table 3 together with the experimental values for comparison. There is a reasonable agreement between the two. Thus, the results obtained employing superposition model support the experimental conclusion that Fe^{3+} ions substitute at Al^{3+} site in the CSA crystal [10].

V. Conclusions

CFPs and ZFSPs for Fe^{3+} ion doped CSA have been determined using superposition model and perturbation theory, respectively. The obtained ZFSPs show a reasonable agreement with the experimental values. The calculated optical spectra are also in reasonable agreement with the experimental ones. The inference found on the basis of superposition model supports the experimental one that Fe^{3+} ions substitute at Al^{3+} site in the CSA crystal.

References

[1]. A. Weil, J. R. Bolton, Electron Paramagnetic Resonance: Elementary Theory and Practical Applications, 2nd ed., Wiley, New York, 2007.

[2]. F. E. Mabbs, D. Collison, D. Gatteschi Electron Paramagnetic Resonance of d Transition Metal Compounds, Elsevier, Amsterdam, 1992.

[3]. D. J. Newman, J. Phys. C: Solid State Phys. **10** (1977) L315-L318.

[4]. M. I. Bradbury, D. J. Newman, Chem. Phys. Lett. **1** (1967) 44-45.

[5]. Y. Y. Yeung, J. Phys. C: Solid State Phys. **21**(1988)2453-61.

[6]. T. H. Yeom, S. H. Choh, M. L. Du, J. Phys.: Condens. Matter **5** (1993) 2017-2024.

[7]. W. L. Yu, Phys. Rev. **B 39** (1989) 622-632.

[8]. M. G. Brik, C. N. Avram, N. M Avram, Physica **B 384** (2006) 78-81.

[9]. Z. Y. Yang, J. Phys.: Condens. Matter   **12** (2000) 4091-4096.

[10]. A. Leble, J. J. Rousseau, G. Courbion, Solid State Commun. 61 (1987)551-554.

[11]. W. L. Yu, M.G. Zhao, Phys. Rev. B **37** (1988) 9254-9267.

[12]. G. Courbion, C. Jacoboni Et R. De Pape, Acta Cryst. B32(1976)3190-3193.

[13]. A. Abragam, B. Bleaney, Electron Paramagnetic Resonance of Transition Ions, Clarendon Press, Oxford, 1970.

[14]. C. Rudowicz, Magn. Reson. Rev. 13 (1987) 1-89.

[15]. C. Rudowicz, H. W. F. Sung, Physica B 300 (2001) 1-26.

[16]. C. J. Radnell, J. R. Pilbrow, S. Subramanian, M. T. Rogers, J. Chem. Phys. 62 (1975) 4948-4952.

[17]. C. Rudowicz, R. Bramley, J. Chem. Phys. 83 (1985) 5192-5197.

[18]. B. N. Figgis, M. A. Hitchman, Ligand Field Theory and its Applications, Wiley, New York, 2000.

[19]. T. H. Yeom, S. H. Choh, M. L. Du and M. S. Jang, Phys. Rev. B 53 (1996) 3415- 3421.

[20]. C. Rudowicz, S. K. Misra, Appl. Spectrosc. Rev. 36 (2001) 11–63.

[21]. Z. Y. Yang, C. Rudowicz, Y. Y. Yeung, Physica B 348 (2004) 151–159.

[22]. Z. Y. Yang, Y. Hao, C. Rudowicz, Y. Y. Yeung, J. Phys.: Condens. Matter 16 (2004) 3481–3494.

[23]. T. H. Yeom, Y. M. Chang, S. H. Choh, C. Rudowicz, Phys. Stat. Sol. b185 (1994) 409–415; C. Rudowicz, Z. Y. Yang, Y. W. Lun, J. Phys. Chem. Solids, 53 (1992) 1227-1236.

[24]. C. K. Jorgensen, Modern Aspects of Ligand Field Theory, North- Holland, Amsterdam, 1971, p.305.

[25]. A. L. Hector, W. Levasan, M. T. Weller, E. G. Hope, J. Fluorine Chem. 84 (1997) 161-165..

[26]. D. J. Newman, B. Ng, Rep. Prog. Phys. 52(1989)699-763.

[27]. D. J. Newman, B. Ng (Eds.), Crystal Field Handbook, Cambridge University Press, Cambridge, 2000.

[28]. D. J. Newman, D. C. Pryce, W. A. Runciman, Am. Miner. 63 (1978) 1278-1281.

[29]. A. Edgar, J. Phys. C: Solid State Phys. 9 (1976) 4303-4314.

[30]. P. Gnutek, Z. Y. Yang and C. Rudowicz, J. Phys.: Condens. Matter 21, 455402 (2009)(11pp).

[31]. Y. Y. Yeung, C.Rudowicz, J. Comput. Phys. 109 (1993) 150-152.

Figure and Table captions:

Fig 1. Crystal structure of CSA with symmetry adopted axis system (SAAS).

Table 1. Atomic coordinates in CSA crystal and bond length R (without and with distortion) together with angle θ, φ (one site).

Table 2. Crystal field parameters and zero field splitting parameters of Fe³⁺ doped CSA single crystal.

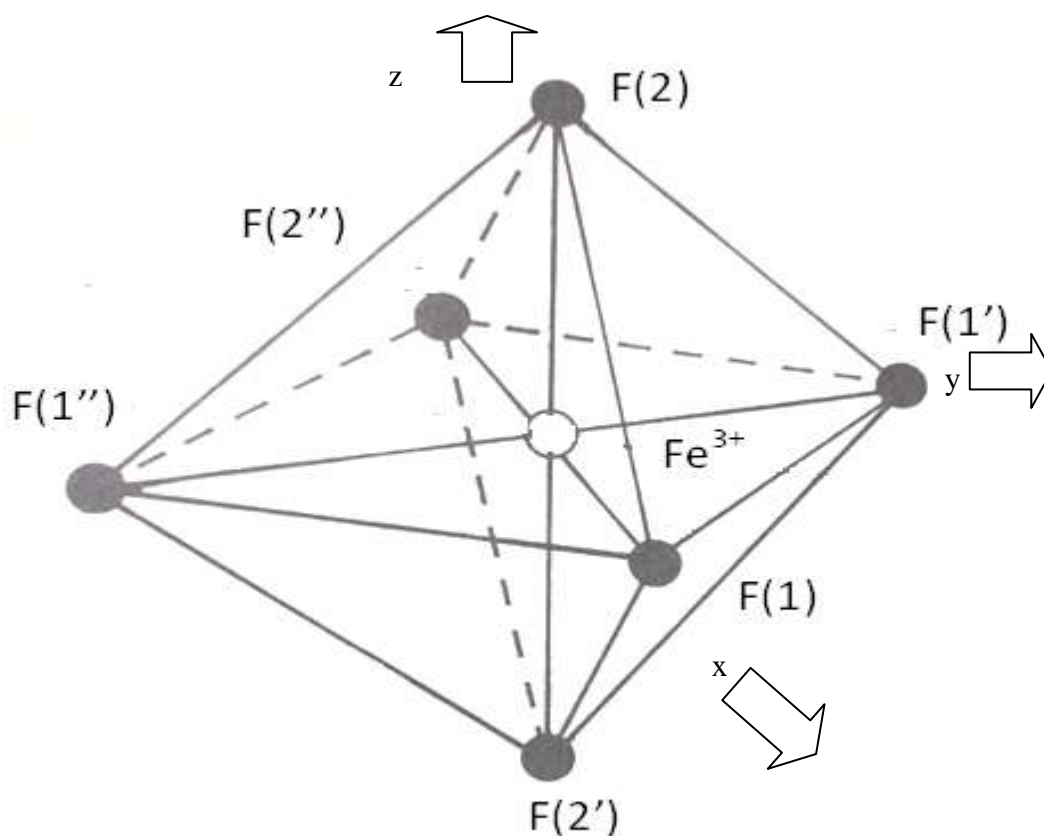Table 3. Experimental and calculated (CFA package) energy band positions of Fe³⁺ doped CSA single crystal.

Fig. 1

Table 1

Position of Fe^{3+}	Ligands				Spherical co-ordinates of ligands		
		x	y	z	R(nm)	θ^0	φ^o
				(Å)			
			Without distortion				
Site I: Substitutional	F(1)	0.2968	0.2968	-0.0768	0.1829 R$_1$	92.40 θ_1	96.38 φ_1
Al^{3+} (0.5000, 0, 0)	F(1')	0.2968	-0.0768	0.2968	0.2043 R$_2$	81.64 θ_2	95.76 φ_2
	F(1")	-0.0768	0.2968	0.2968	0.3546 R$_3$	85.19 θ_3	99.39 φ_3
	F(2")	0.3828	-0.0847	-0.0847	0.1747 R$_4$	92.77 θ_4	93.84 φ_4
	F(2)	-0.0847	-0.0847	0.3828	0.3820 R$_5$	84.25 θ_5	98.84 φ_5
	F(2')	-0 0847	0.3828	-0.0847	0.3820 R$_6$	91.27 θ_6	98.80 φ_6
			With distortion				
	F(1)				0.2919 R$_1$+ΔR$_1$		
	F(1')				0.3043 R$_2$+ΔR$_2$		
	F(1")				0.4545 R$_3$+ΔR$_3$		
	F(2")				0.2747 R$_4$+ΔR$_4$		
	F(2)				0.4818 R$_5$+ΔR$_5$		
	F(2')				0.4818 R$_6$+ΔR$_6$		

Table 2

| Site | R_0(nm) | Crystal- field parameters (cm⁻¹) | | | | | Zero-field splitting parameters ($\times 10^{-4}$cm⁻¹) | | |
		B_{20}	B_{22}	B_{40}	B_{42}	B_{44}	$|D|$	$|E|$	$|E|/|D|$
Without distortion									
Site I $\overline{\dfrac{A_2}{A_4}}$=10	0.108	-6767.33	-8226.38	615.8491	645.3895	4650.557	1789	788	0.440
With distortion									
Site I $\overline{\dfrac{A_2}{A_4}}$=10	0.108	-2166.79	-1748.37	69.45583	72.81262	4240.259	682.2	104.2	0.152
						Exp.	682.0	640.3	0.938

Table 3

Transition from $^6A_{1g}(S)$	Observed wave number (cm⁻¹)	Calculated wave number (cm⁻¹)
$^4T_{1g}(G)$	16300	
$^4T_{2g}(G)$	22000	
$^4A_{1g}(G)$	25100	24451, 24472
$^4E_g(G)$	26750	26714, 26726, 26752, 26766
$^4T_{2g}(D)$	29600	28805, 28831, 29063, 29116, 30376, 30512
$^4E_g(D)$	31850	31483, 31605, 31820, 31865
$^4T_{1g}(P)$	37050	37478, 37580, 37651, 37778, 37947, 38764
$^4T_{1g}(F)$	42550	42122, 42332, 42387, 42538, 42842, 43046
$^4T_{2g}(F)$	46750	46079, 46320, 46493, 46846, 46958, 46993